Multidecadal Changes in the Relationship between ENSO and Wet-Season Precipitation in the Arabian Peninsula

IN-SIK KANG

School of Earth and Environmental Sciences, Seoul National University, Seoul, South Korea, and Center of Excellence for Climate Change Research, Department of Meteorology, King Abdulaziz University, Jeddah, Saudi Arabia

IRFAN UR RASHID

Center of Excellence for Climate Change Research, Department of Meteorology, King Abdulaziz University, Jeddah, Saudi Arabia

FRED KUCHARSKI

International Centre for Theoretical Physics, Trieste, Italy, and Center of Excellence for Climate Change Research, Department of Meteorology, King Abdulaziz University, Jeddah, Saudi Arabia

MANSOUR ALMAZROUI AND ABDULRAHMAN K. ALKHALAF

Center of Excellence for Climate Change Research, Department of Meteorology, King Abdulaziz University, Jeddah, Saudi Arabia

(Manuscript received 23 May 2014, in final form 6 March 2015)

ABSTRACT

Multidecadal variations in the relationship between El Niño–Southern Oscillation (ENSO) and the Arabian Peninsula rainfall are investigated using observed data for the last 60 years and various atmospheric general circulation model (AGCM) experiments. The wet season in the Arabian Peninsula from November to April was considered. The 6-month averaged Arabian rainfall was negatively correlated with ENSO for an earlier 30-yr period from 1950 to 1979 and positively correlated to ENSO for a more recent period from 1981 to 2010. The multidecadal variations can be attributed to the variations in Indian Ocean SST anomalies accompanied by ENSO. In the early 30-yr period, ENSO accompanied relatively large SST anomalies in the Indian Ocean, whereas in the recent 30-yr period it accompanied relatively small SST anomalies in the Indian Ocean. The atmospheric anomalies in the Arabian region during ENSO are combined responses to the Pacific and Indian Ocean SST anomalies, which offset each other during ENSO. The recent El Niño events accompanied negative 200-hPa geopotential height (GH) anomalies over the Arabian region, mainly forced by the Pacific SST anomalies, resulting in an increase of precipitation over the region. In contrast, in the early 30-yr period, Indian Ocean SST anomalies played a dominant role in the atmospheric responses over the Arabian region during ENSO, and the negative GH anomalies and more precipitation over the Arabian region were mainly forced by the negative SST anomalies over the Indian Ocean, which appeared during La Niña. These observed findings are confirmed by various AGCM experiments.

1. Introduction

El Niño–Southern Oscillation (ENSO) has been known to considerably influence the global climate, particularly over most parts of the tropics (Horel and Wallace 1981), the Pacific–North American region (Wallace and Gutzler 1981), and the Asian monsoon region (e.g., Rasmusson and Carpenter 1983; Webster and Yang 1992; Ju and Slingo 1995; Wang et al. 2004). For regional climate predictions, knowledge of the ENSO connection to a regional climate is important, as most climate prediction signals in current operational prediction systems arise from ENSO (e.g., Palmer et al. 2004; Wang et al. 2009). However, there has been a lack of studies on the impact of ENSO on precipitation over

Corresponding author address: Prof. In-Sik Kang, School of Earth and Environmental Sciences, Seoul National University, Seoul 151-747, South Korea.
E-mail: kang@climate.snu.ac.kr

DOI: 10.1175/JCLI-D-14-00388.1

the Arabian Peninsula (AP). This study aims to investigate the relationship between interannual variations in the AP precipitation and global SST anomalies, particularly ENSO, and how the relationship between ENSO and the AP precipitation anomalies has been changed over the last 60 years.

The region bounded by North Africa and the Arabian Peninsula is covered by the world's largest desert. Although this region is arid, it experiences substantial variations in rainfall with interannual and interdecadal time scales (Zeng and Yoon 2009; Kucharski et al. 2013b), and overall precipitation over the Arabian Peninsula has a decreasing trend in recent decades (Almazroui et al. 2012). A number of studies have investigated precipitation variability in the Sahel region, particularly focused on its linkage to the SST anomalies over the Atlantic and Indian Oceans as well as ENSO (e.g., Folland et al. 1986; Rowell et al. 1995; Giannini et al. 2003; Bader and Latif 2003; Hagos and Cook 2008; Mohino et al. 2011; Feudale and Kucharski 2013). These studies have demonstrated that the precipitation variability in the arid region, although relatively small in size, has been sensitively responding to global SST fluctuations.

The ENSO teleconnection to remote regional precipitations is known to have decadal variations, particularly in the Indian region (e.g., Torrence and Webster 1999; Krishna Kumar et al. 1999; Krishnamurthy and Goswami 2000; Kinter et al. 2002; Annamalai and Liu 2005; Gershunov et al. 2001). Many previous studies have demonstrated that the Indian summer monsoon (ISM) was negatively correlated to ENSO in the 1960s–70s but this correlation has been weak in the more recent period after 1980 (e.g., Krishna Kumar et al. 1999; Kucharski et al. 2007; Kinter et al. 2002). Turner et al. (2007) and Annamalai et al. (2007) showed that this variation in the ENSO–Indian monsoon relationship is not related to the anthropogenic global warming but rather results from internal variations of ocean–atmosphere coupled system over the globe. Kumar et al. (2007) claimed that the ENSO teleconnection in the Indian region depends on the zonal position of the ENSO SST anomalies in the Pacific Ocean. Webster et al. (1999), on the other hand, demonstrated that the Indian Ocean SST state plays a key role in the ENSO–ISM relationship, meaning that Indian Ocean SST anomalies can reinforce or offset the Indian precipitation anomalies directly teleconnected to ENSO.

In contrast to a large number of studies on the ENSO–ISM relationship, the change in the ENSO impact on the Indian ''winter'' monsoon (IWM) has received little attention within the research community. Only a few researchers have studied the ENSO–IWM precipitation relationship in recent years (Kumar et al. 2007; Yadav et al. 2010). In particular, Yadav et al. (2010) showed that the ENSO–IWM relationship was weak in the earlier period between 1950 and 1980, but this relationship has substantially increased in the recent period after 1980, particularly over the northwestern region of India and Pakistan. Yadav et al. (2010) claimed that the increased relationship between the northwest Indian rainfall and ENSO is due to the Pacific SST anomalies, which have intensified for recent El Niño events. Yadav et al. (2009) also showed that the IWM has been also influenced by the North Atlantic Oscillation (NAO); this influence has changed such that the NAO's influence has decreased for the last 50 years but ENSO's influence has increased for the same period. Recently a few papers have shown that the ENSO teleconnections are not stationary and vary at multidecadal time scales in phase with the Atlantic multidecadal oscillation (AMO) (e.g., Martín-Rey et al. 2014; Kang et al. 2014). For the Sahel, for example, the presence of Pacific anomalies together with opposite-in-sign anomalies in the Atlantic have been pointed out as an important contributor for the changes in the Sahel–ENSO relationship after the 1970s, together with the multidecadal modulations (Losada et al. 2012). Also, other papers have pointed out the nonstationary influence of ENSO in European rainfall (e.g., Greatbatch et al. 2004; López-Parages and Rodríguez-Fonseca 2012; López-Parages et al. 2013), indicating how the influence of the changes in the background state is a determining factor for the different responses over Europe.

The winter regional climates over the Middle East, located to the north of the Indian Ocean and the east of Sahel, are expected to be influenced by ENSO, and the ENSO teleconnection may be modulated with multidecadal time scales, as seen in other regions near the Middle East. In the present study, we investigate the global SST anomaly patterns associated with the precipitation anomalies averaged over the Arabian Peninsula during the wet season, which is from November to April (Almazroui 2011). We also investigate how the teleconnected global SST patterns have changed over the last 60 years from 1950 to 2010 and how these changes have influenced the ENSO–AP precipitation relationship. Section 2 describes the data and the model used in the present study. The results obtained from the observed data are provided in section 3. In section 4, the observed findings are supported by the model experiments. A summary and some concluding remarks are provided in section 5.

2. Data and model

The precipitation data over the Arabian region was obtained from the monthly-mean Global Precipitation Climatology Centre (GPCC; Schneider et al. 2014)

dataset, which is available for the period of 1901–2010. The spatial resolution of the GPCC precipitation data is 0.5° × 0.5° in longitude and latitude. The monthly mean SST data used were obtained from the National Oceanic and Atmospheric Administration (NOAA) Extended Reconstructed SST (ERSST V.3; Smith et al. 2008), whose data period covers the period from 1854 to the present. The spatial resolution of the SST dataset is 2° × 2° in longitude and latitude. The data quality of both datasets is questionable for the period before the early twentieth century because the gridded datasets were obtained from a relatively small number of stations for that early period (Schneider et al. 2014; Smith and Reynolds 2003; Smith et al. 2008). The monthly-mean 200-hPa geopotential height data were obtained from the National Centers for Environmental Prediction (NCEP)–National Center for Atmospheric Research (NCAR) reanalysis dataset (Kalnay et al. 1996), which is available from 1948 to the present. The spatial resolution is 2.5° × 2.5° in longitude and latitude. Considering the data quality and the common data period, we used the observed data for the period 1950–2010. The annual total precipitation over the Arabian region is dominated by rainfall for the wet season, from November to April. All climate statistics used in the present study are the average for the 6-month period from November to April.

The model used is the atmospheric general circulation model (AGCM) developed at the International Center for Theoretical Physics (ICTP), referred to as the "SPEEDY" AGCM (Kucharski et al. 2013a). This model was described by Molteni (2003) in its five-level version and by Kucharski et al. (2006) in its current eight-level version. The model has a spectral dynamical core (Held and Suarez 1994) and parameterized physical processes including shortwave and longwave radiation, large-scale condensation, convection, and surface fluxes of momentum, heat, and moisture. Convection is represented by a mass-flux scheme that is activated when conditional instability is present. Boundary layer fluxes are calculated by a stability-dependent bulk formula. Land and sea ice temperatures are determined by a simple one-layer thermodynamic model. The AGCM used in the present study is configured with eight vertical levels and with a spectral truncation at rhomboidal wavenumber 30.

Three sets of ensemble simulations were performed:

(i) a nine-member ensemble forced globally by the observed SST (denoted as C20C) for the last 60 years;
(ii) a nine-member ensemble forced by the observed SST in the Pacific Ocean region (from 120°E to the coast of South America) and elsewhere by climatologically varying monthly mean (no interannual variation) SST (Exp-PAC); and
(iii) a nine-member ensemble forced by the observed SST in the Indian Ocean region (from the coast of Africa to 120°E) and elsewhere by climatological varying monthly mean SST (Exp-IND).

All simulations start in 1948 and are integrated to the end of 2010. Different ensemble members are created by slightly different initial conditions. The first two years of the integrations are considered as a spinup period; therefore, all simulations are analyzed from 1950 onward.

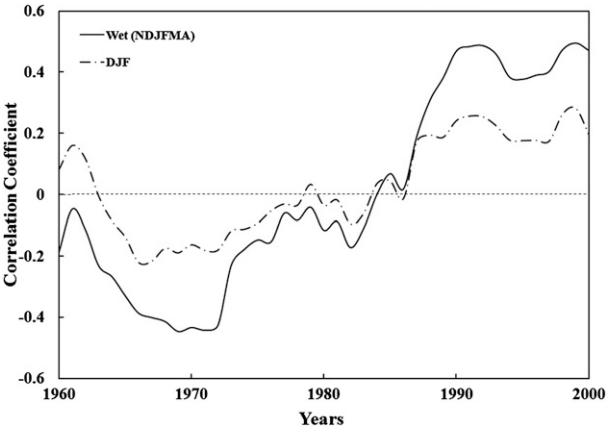

FIG. 1. 21-yr sliding correlation between the Arabian Peninsula (AP) rainfall and Niño-3.4 SST index for the period 1950–2010. The continuous and dashed lines indicate the correlations for the 6-month wet season and the DJF season, respectively.

3. Results from observed data

The monthly-mean precipitation data for the grids of the Arabian Peninsula region were extracted from the GPCC dataset. The region covers the whole AP up to the northern boundary at 30°N. In the present study, the 6-month wet season average of the AP regional mean precipitation is used as a reference time series, which will be denoted as the AP time series. First, we examined the relationship between the AP time series and ENSO. The Niño-3.4 index, which is the SST averaged for the domain of 5°N–5°S, 120°–170°W and averaged for the corresponding six months, is used for representing the ENSO state. The simultaneous correlation between the two time series is 0.1 for the entire 60-yr period. However, it is 0.51 for the recent 30-yr period of 1981–2010, which is statistically significant with a 95% confidence level, indicating that the ENSO relationship has changed for the last 60-yr period. To observe the changes, sliding correlations have been made with a 21-yr window (Fig. 1). As seen in Fig. 1, the correlation was negative for the 1960s and 1970s and increased after the early 1980s, and its value reached at the maximum value

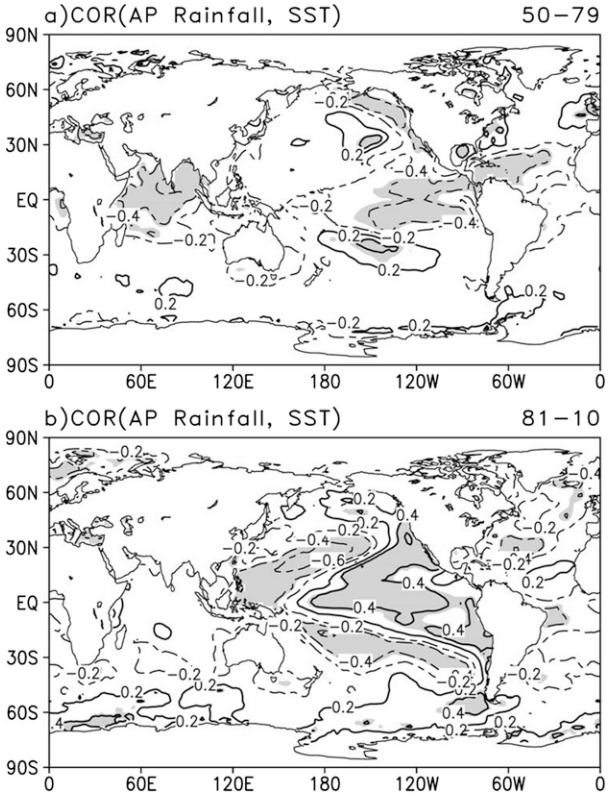

FIG. 2. Correlation maps between the Arabian Peninsula rainfall and global SSTs for the 30-yr periods of (a) 1950–79 and (b) 1981–2010. The variables used are the 6-month average for November–April.

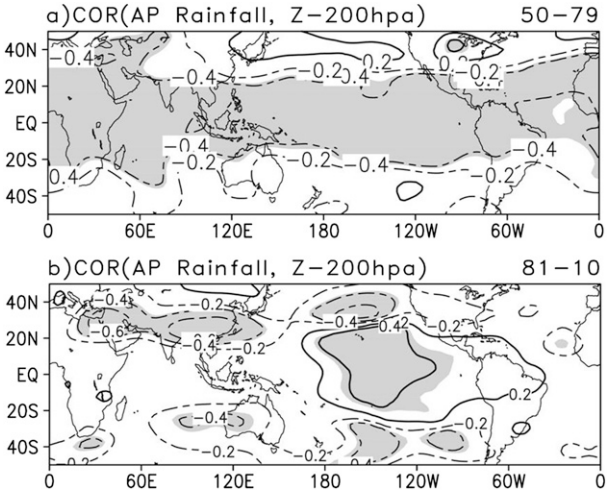

FIG. 3. Correlation maps between the Arabian Peninsula rainfall and 200-hPa geopotential height for the domain between 50°S and 50°N for the 30-yr periods of (a) 1950–79 and (b) 1981–2010.

close to 0.5 in the early 1990s and then maintained the value afterward. It is interesting to note that the sign of the correlation has changed in the period from the late 1970s to the early 1980s, when the global climate, particularly over the Pacific, experienced a climate shift (Graham 1994). One may be interested in seeing the multidecadal changes of the correlation by separating the period into winter [December–February (DJF)] and spring [March–May (MAM)] seasons. The results for each season are similar to those shown in Fig. 1, except that the correlation value is slightly smaller as indicated by a dashed line in Fig. 1 for the DJF season.

Figure 2 shows the spatial distribution of the correlation coefficient between the AP precipitation time series and the corresponding global SST for the 30-yr periods of (a) 1950–79 and (b) 1981–2010. In the figures, the shading indicates the region of statistical significance at 95% confidence level. The Student's *t* test is used for the statistical significance. A striking feature of Fig. 2 is that the correlations have opposite signs in the central and eastern tropical Pacific during the two periods, confirming the above statements relating to Fig. 1. Also noted is that the AP precipitation is correlated not only with the SSTs in the ENSO region but also with the SSTs in other ocean regions. In the 1950–79 period, the AP precipitation is negatively correlated with the SSTs in most of the tropical oceans, particularly in the tropical Indian Ocean. However, for the period of 1981–2010 (Fig. 2b), the correlation between the AP precipitation and the Indian Ocean SSTs has almost disappeared. These results indicate that the SST anomaly patterns influencing the AP precipitation anomalies have been significantly changed for the last 60 years.

It is difficult to understand such a large change in the correlation (from negative to positive) between the AP precipitation and ENSO for the last 60-yr period. To investigate this issue, we examined the 200-hPa geopotential height (GH) anomalies associated with the AP rainfall fluctuations for those two 30-yr periods. Figures 3a and 3b shows the correlation maps between the AP precipitation and the 200-hPa GH for 1950–79 and 1981–2010, respectively. Interestingly, most of the tropics are covered by the negative correlations for the early 30 years, but significant positive correlations are confined to the tropical eastern Pacific in the latter 30 years. However, in the two figures the same sign of correlations appears in the subtropical Asian region from the subtropical western Pacific to the AP, indicating that the AP precipitation anomalies in the boreal winter are associated with the upper-tropospheric cyclonic circulation anomalies over the region. Also noted is that the correlation values over the central Arabian Peninsula were increased from −0.4 (in the earlier period) to −0.7 in the latter period. The increase of AP rainfall associated with the local upper-tropospheric cyclonic circulation anomalies is related

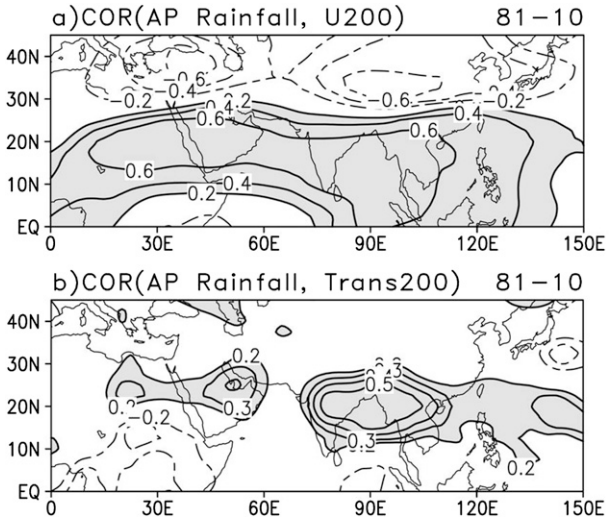

FIG. 4. Correlation maps between the AP rainfall and 200-hPa (a) zonal wind and (b) transient activity anomaly of the wet season for the period of 1981–2010. Shading indicates the absolute value of correlation coefficient larger than 0.2.

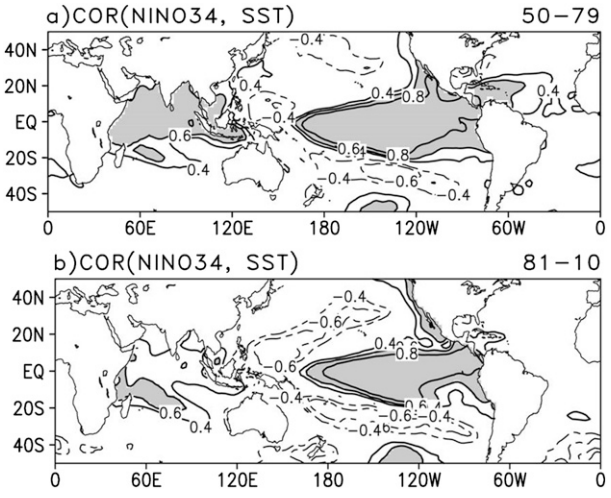

FIG. 5. Correlation maps between the Niño-3.4 index and SSTs for the 30-yr periods of (a) 1950–79 and (b) 1981–2010.

to the shift of the Arabian jet stream to the central Arabian Peninsula, particularly in the recent period, as seen in Fig. 4a. The intensified upper-level zonal wind causes more frequent passages of transients over the region (Fig. 4b), resulting in more precipitation in the region for the recent period 1981–2010. The transient activity shown in Fig. 4b is calculated in terms of the root-mean-square of the synoptic transients (2–10-day filtered 200-hPa geopotential height) for a wet season (e.g., Kang et al. 2011; Abid et al. 2015, manuscript submitted to *J. Climate*). Similar characteristics appeared in the earlier period although the correlation patters were somewhat weaker than those of the recent period. It is also pointed out that the direct effect of cyclonic circulation anomalies (Fig. 3a), which enhance moisture convergence, appears to be more important for regional precipitation anomalies in the earlier period. Also note that the AP precipitation anomaly is associated with the negative upper-level GH anomaly in the AP region, which has been linked to the negative GH anomalies in the whole tropics in the early 30-yr period (Fig. 3a) but to the positive anomalies in the tropical eastern Pacific for the latter 30-yr period (Fig. 3b). The different linkage of the AP rainfall to the tropical Pacific is further investigated in terms of the multidecadal changes in the global SST and upper-level circulation anomaly patterns associated with ENSO.

The global SST anomalies associated with ENSO for the earlier and later 30-yr periods are shown in Figs. 5a and 5b, respectively. The most distinctive difference between the two figures appears in the tropical Indian Ocean, particularly to the north of the equator, where the correlation values are over 0.6 in Fig. 5a but between 0.1 and 0.5 in Fig. 5b. Therefore, the earlier ENSO episodes accompanied large SST anomalies in the whole tropical Indian Ocean, whereas the ENSOs in the latter period accompanied relatively small SST anomalies in the northern Indian Ocean. The same is true for the tropical Atlantic Ocean. As a result, the earlier El Niño (La Niña) events accompanied more extensive warming (cooling) in the entire tropics, but the SST anomalies in the latter period are more or less confined to the tropical Pacific. The corresponding upper-tropospheric GH anomaly patterns are shown in Figs. 6a and 6b. For both periods, the 200-hPa GH anomalies are positively

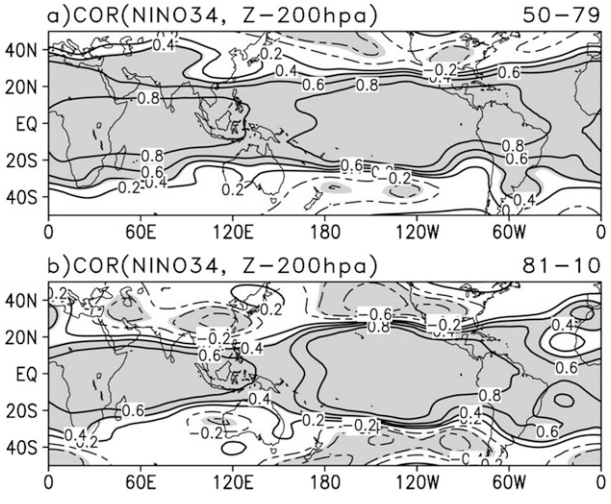

FIG. 6. Correlation maps between the Niño-3.4 index and 200-hPa geopotential height for the 30-yr periods of (a) 1950–79 and (b) 1981–2010.

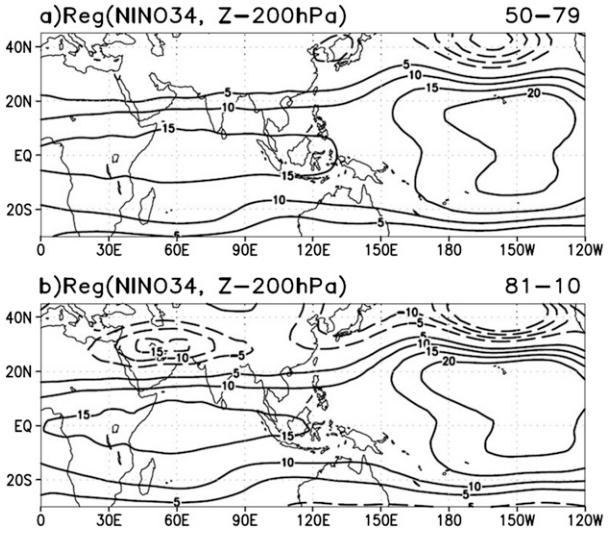

FIG. 7. Regression maps of 200-hPa geopotential height anomalies against the normalized Niño-3.4 index, obtained from the AGCM simulation with prescribed SST boundary conditions observed for (a) 1950–79 and (b) 1981–2010. The regression value is obtained using the covariance of the two variables divided by the root-mean-square of the Niño-3.4 index.

correlated with ENSO in the entire tropics, although the positive correlations are stronger in the earlier period. The large differences between the two figures appear in the subtropical region, particularly in South Asia and the Middle East. In the more recent 30-yr period, the positive correlation is confined to the tropical Indian Ocean (Fig. 6b), whereas it is expanded to the subtropical Indian subcontinent and the Middle East in the early 30-yr period (Fig. 6a). It is important to note that the GH anomalies in the Middle East are negatively correlated with ENSO during the recent 30-yr period but positively correlated with ENSO during the earlier period. Therefore, the positive AP precipitation associated with the local negative upper-level GH anomalies is accompanied by La Niña in the early 30-yr period but by El Niño in the recent period. Figure 5 indicates that such differences appear to be related to the differences in the Indian Ocean SST anomalies associated with ENSO for the two different 30-yr periods.

4. Model results

In this section, we have performed several AGCM experiments to support the observed findings in the previous section. First, we examined how the ENSO teleconnection has been changed for the last 60 years using the AGCM experiment with prescribed SST boundary conditions for the last 60 years (the experiments similar to the C20C experiment; Folland et al. 2002). Figures 7a and 7b show the correlation maps between the Niño-3.4 index and the simulated 200-hPa GH anomalies for the 30-yr periods of 1950–79 and 1981–2010, respectively. Figure 7b is similar to Fig. 6b, indicating that the AGCM is able to reproduce the observed ENSO teleconnection for the recent 30 years reasonably well, particularly the strong negative GH anomalies in the Arabian region during El Niño. For the early 30-yr period, the positive GH anomalies in the South Asian region are actually expanded slightly to the north compared to those of Fig. 7b, as in observation, but the expansion is not as much as that of the observation (Fig. 6a), and the GH anomalies in the AP region have a small positive value in Fig. 7a. It is noted that a big difference between the two figures appears in the subtropical Asian region, including the Middle East and the Far East. In the northern subtropics, the negative GH anomalies are confined in the eastern Pacific in Fig. 7a, whereas in Fig. 7b those negative anomalies appear in most of the northern subtropical region from the eastern Pacific all the way to the AP region. It is also noted that the GH responses in the eastern Pacific in the recent period are slightly larger than those in the early period, since the ENSO amplitudes have increased for the last 50 years (Kang et al. 2006; Ehsan et al. 2013). As mentioned above, in the early 30-yr period, the simulated GH anomalies over the Arabian Peninsula region associated with ENSO are much weaker than the observed. This discrepancy may be due to the lack of air–sea coupling of the AGCM simulations in the Indian Ocean and/or the land feedback process, which is not well represented in the model. Nevertheless, the model experiments clearly demonstrate that the multidecadal change in the ENSO teleconnection over the AP region is due to the changes in ENSO-related SST boundary conditions in the ocean basins including the Pacific and Indian Oceans.

To identify the contributions of each basin's (Pacific and Indian Oceans separately) SST anomalies to the 200-hPa teleconnection anomalies, we performed two additional AGCM experiments, whose experimental setting was the same as reported above, but with the observed SST anomalies in the Pacific only (Exp-PAC) and in the Indian Ocean only (Exp-IND). Details of the experiments can be found in section 2. Figures 8a and 8b are the regression maps of 200-hPa GH with respect to the normalized Niño-3.4 index, obtained with the Exp-PAC, for the earlier and latter 30-yr periods, respectively. Thus, the figures show the 200-hPa GH anomalies forced by the Pacific component of the ENSO SST anomalies during each 30-yr period. Both figures are characterized by the positive anomalies in the tropics and the negative anomalies in the northern subtropics. The most distinctive difference between the

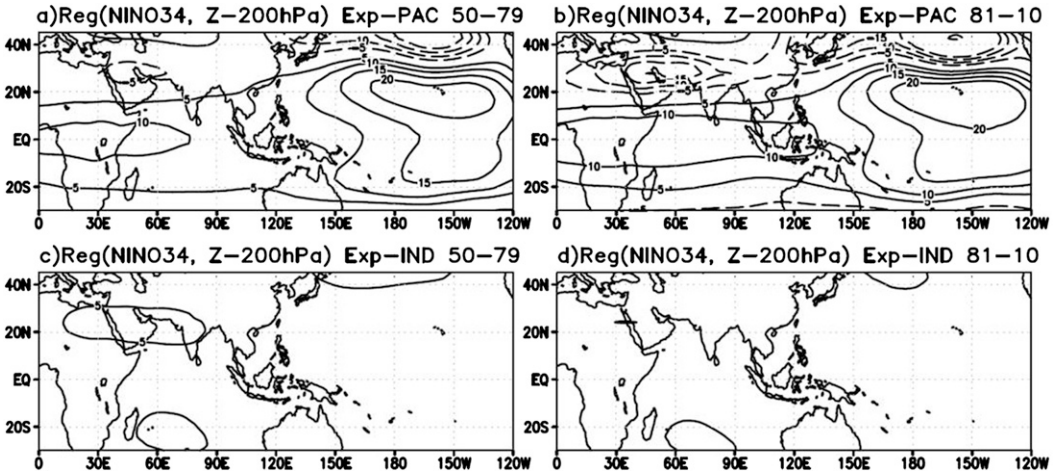

FIG. 8. As in Fig. 5, but for the AGCM simulation with the SST anomalies (a),(b) for the Pacific only and (c),(d) with the Indian Ocean only; (a) and (c) are for 1950–79 and (b) and (d) for 1981–2010.

two figures is found in the region from northeastern Africa to the subtropical Asian continent, centered at the Arabian Peninsula. For the case of the Exp-IND, the regression maps of 200-hPa GH with respect to the normalized Niño-3.4 index shown in Figs. 8c and 8d illustrate that both figures have a similar spatial pattern but the magnitudes in Fig. 8c are larger than those of Fig. 8d. The reason for this is that ENSOs in the recent 30-yr period have accompanied relatively large SST anomalies in the Indian Ocean compared with those of ENSOs in the earlier 30-yr period, as seen in Fig. 5. It is important to note that the GH response to the Indian Ocean SST anomalies offsets the GH response to the Pacific SST anomalies, particularly in the region from North Africa to northern India. As a result, the total GH anomalies over the Arabian Peninsula region shown in Fig. 7a are very small for the early 30-yr period. Figure 8 also shows that except in the Middle East during the early 30-yr period, the teleconnected GH responses over the globe to ENSO are mainly forced by the Pacific SST anomalies.

Finally, the Indian Ocean impact on the precipitation over the Arabian region is examined using the data from Exp-IND. Figures 9a and 9b show the correlation maps between the rainfall averaged over the Arabian Peninsula region and the SST anomalies over the Indian Ocean for the periods of 1950–79 and 1981–2010, respectively. Both figures show that the Arabian Peninsula rainfall during the wet season is negatively correlated to the Indian Ocean SST anomalies, regardless of the period. The correlation value of 95% statistical significance is 0.36 for the 30-yr period, and therefore the statistically significant correlations cover a large part of the Indian Ocean in both figures. This result indicates that the ENSO–AP rainfall relationship has been changed for the last 60 years because of the change in the relationship between ENSO and Indian Ocean SST anomalies, as shown in Fig. 5. More specifically, during the period 1950–79, ENSO accompanied relatively large SST anomalies in the Indian Ocean, and the negative Indian Ocean SST anomalies accompanied by La Niña produced positive rainfall anomalies in the Arabian Peninsula region; therefore, the Arabian rainfall was negatively correlated with ENSO. During the recent 30-yr period, on the other hand, the SST anomalies in the northern Indian Ocean were not significantly affected by ENSO, and during ENSO the Pacific SST anomalies directly influenced the atmospheric circulation over the Middle East. The El Niño Pacific SST anomalies have forced the negative upper-level GH anomalies over the Middle East, which pushed the subtropical jet stream to the Arabian Peninsula, resulting in more transients and more precipitation in the region. This is why ENSO and Arabian Peninsula precipitation were positively correlated for the recent 30-yr period.

5. Summary and concluding remarks

Multidecadal changes of the relationship between ENSO and Arabian Peninsula rainfall have been investigated using both observed data for the last 60-yr period and various AGCM experiments. The season considered in the present study is the wet season in the Arabian Peninsula for the 6-month period from November to April, and all variables used are the 6-month average. The Arabian rainfall was negative correlated with ENSO for the early 30-yr period of 1950–79 and positively correlated with ENSO for the recent period of

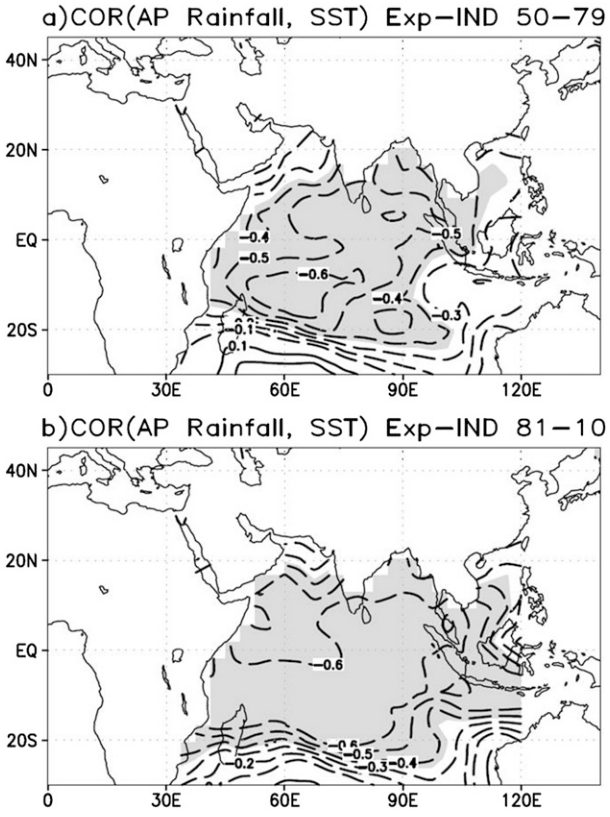

FIG. 9. Correlation maps between the simulated rainfall averaged over the Arabian Peninsula region (12°–32°N, 35°–60°E) and the SST anomalies for the 6-month wet season, for (a) 1950–79 and (b) 1981–2010. The data used are from the AGCM experiment prescribed with the observed SSTs in the Indian Ocean only (Exp-IND). Shading indicates the region of statistical significance at 95% confidence level.

1981–2010. This multidecadal change in the relationship between the Arabian rainfall and ENSO is due to the changes of Pacific and Indian Ocean SST anomalies accompanied with ENSO. In particular, in the early 30-yr period, ENSO had accompanied relatively large SST anomalies in the Indian Ocean, whereas for the more recent 30-yr period ENSO has accompanied large SST anomalies in the Pacific and relatively small SST anomalies in the Indian Ocean. It is found that the atmospheric anomalies in the Arabian Peninsula region during ENSO resulted from the combined responses to the Pacific and Indian Ocean SST anomalies, which offset each other during ENSO, particularly during the earlier period. The recent El Niño events accompanied negative 200-hPa geopotential height anomalies over the Arabian Peninsula region, mainly forced by the Pacific SST anomalies. These negative GH anomalies pushed the subtropical jet stream to the Arabian Peninsula, resulting in an increase of transients and more precipitation over the region. On the other hand, in the earlier 30-yr period of 1950–79, the Indian Ocean SST anomalies played a dominant role in the atmospheric responses over the Middle East during ENSO, and the negative GH anomalies and more precipitation over the Arabian Peninsula region was mainly forced by the negative SST anomalies over the Indian Ocean, which were associated with La Niña.

The observed findings mentioned above are confirmed by various AGCM experiments. In particular, the Arabian Peninsula rainfall is negatively correlated with the Indian Ocean SST anomalies in the AGCM experiment with the observed SST anomalies confined only to the Indian Ocean, whereas it is positively correlated with the ENSO SST anomalies in the experiment with the SST anomalies only in the Pacific Ocean. Therefore, ENSO's impact on the Arabian Peninsula climate strongly depends on the magnitude of the Indian Ocean SST anomalies for the ENSO period. The Indian Ocean SST anomalies did not play an important role in the ENSO teleconnection anomalies over the Middle East for the recent 30 years but played a significant role for the early 30-yr period. It is noted that in the AGCM experiments the atmospheric responses over the Middle East to the Indian Ocean SST anomalies appear to be relatively small compared to the observed counterpart. This weak response may be due to the lack of air–sea interaction over the Indian Ocean and a poor representation of land feedback processes over the arid region.

It is also worth mentioning that the multidecadal changes of ENSO teleconnection presented in this study may be associated with the global climate shift that occurred during the late 1970s and early 1980s (Graham 1994). Recent studies also suggested that ENSO can be modulated by the Atlantic multidecadal oscillation (AMO) (Dong et al. 2006; Timmermann et al. 2007; Rodríguez-Fonseca et al. 2009; López-Parages and Rodríguez-Fonseca 2012; Keenlyside et al. 2013; Kang et al. 2014). In particular, Kang et al. (2014) demonstrated that the ENSO modulation is due to changes of the basic state in the tropical Pacific, influenced by the AMO. The AMO may also influence the Indian Ocean basic state and thus the ENSO teleconnection to the Indian Ocean and surrounding continental regions. Losada et al. (2010) has studied the modulation of ENSO teleconnection associated with the AMO using AGCMs, but further studies using coupled GCMs would be needed as in Kang et al. (2014). Also, further studies are needed to clarify the relationship between the climate shift in late 1970s and the changes in global ENSO teleconnection.

Acknowledgments. The present study was supported by the Center of Excellence for Climate Change Research, King Abulaziz University, Jeddah, Saudi Arabia, and the National Research Foundation of Korea grant funded by the South Korean government (MEST) (NRF-2012M1A2A2671775) and the BK21 program. The Abdus Salam International Centre for Theoretical Physics (ICTP), Trieste, Italy, is also acknowledged for providing the analysis of the SPEEDY MODEL results. The authors also thank three anonymous reviewers for their useful comments to improve the manuscript.

REFERENCES

Almazroui, M., 2011: Calibration of TRMM rainfall climatology over Saudi Arabia during 1998–2009. *Atmos. Res.,* **99,** 400–414, doi:10.1016/j.atmosres.2010.11.006.

——, M. Nazrul Islam, H. Athar, P. D. Jones, and M. A. Rahman, 2012: Recent climate change in the Arabian Peninsula: Annual rainfall and temperature analysis of Saudi Arabia for 1978–2009. *Int. J. Climatol.,* **32,** 953–966, doi:10.1002/joc.3446.

Annamalai, H., and P. Liu, 2005: Response of the Asian summer monsoon to changes in El Niño properties. *Quart. J. Roy. Meteor. Soc.,* **131,** 805–831, doi:10.1256/qj.04.08.

——, K. Hamilton, and K. R. Sperber, 2007: The South Asian summer monsoon and its relationship with ENSO in the IPCC AR4 simulations. *J. Climate,* **20,** 1071–1092, doi:10.1175/JCLI4035.1.

Bader, J., and M. Latif, 2003: The impact of decadal-scale Indian Ocean sea surface temperature anomalies on Sahelian rainfall and the North Atlantic Oscillation. *Geophys. Res. Lett.,* **30,** 2169, doi:10.1029/2003GL018426.

Dong, B., R. T. Sutton, and A. A. Scaife, 2006: Multidecadal modulation of El Niño–Southern Oscillation (ENSO) variance by Atlantic Ocean sea surface temperatures. *Geophys. Res. Lett.,* **33,** L08705, doi:10.1029/2006GL025766.

Ehsan, M. A., I.-S. Kang, M. Almazroui, M. A. Abid, and F. Kucharski, 2013: A quantitative assessment of changes in seasonal potential predictability for the twentieth century. *Climate Dyn.,* **41,** 2697–2709, doi:10.1007/s00382-013-1874-x.

Feudale, L., and F. Kucharski, 2013: A common mode of variability of African and Indian monsoon rainfall. *Climate Dyn.,* **41,** 243–254, doi:10.1007/s00382-013-1827-4.

Folland, C. K., T. N. Palmer, and D. E. Parker, 1986: Sahel rainfall and worldwide sea temperatures. *Nature,* **320,** 602–607, doi:10.1038/320602a0.

——, J. Shukla, J. Kinter, and M. J. Rodwell, 2002: The climate of the twentieth century project. *CLIVAR Exchanges,* No. 7, CLIVAR International Project Office, Southhampton, United Kingdom, 37–39.

Gershunov, A., N. Schneider, and T. Barnett, 2001: Low-frequency modulation of the ENSO–Indian monsoon rainfall relationship: Signal or noise? *J. Climate,* **14,** 2486–2492, doi:10.1175/1520-0442(2001)014<2486:LFMOTE>2.0.CO;2.

Giannini, A., R. Saravanan, and P. Chang, 2003: Oceanic forcing of Sahel rainfall on interannual to interdecadal time scales. *Science,* **302,** 1027–1030, doi:10.1126/science.1089357.

Graham, N. E., 1994: Decadal-scale climate variability in the tropical and North Pacific during the 1970s and 1980s: Observations and model results. *Climate Dyn.,* **10,** 135–162, doi:10.1007/BF00210626.

Greatbatch, R. J., J. Lu, and K. A. Peterson, 2004: Nonstationary impact of ENSO on Euro-Atlantic winter climate. *Geophys. Res. Lett.,* **31,** L02208, doi:10.1029/2003GL018542.

Hagos, S. M., and K. H. Cook, 2008: Ocean warming and late-twentieth-century Sahel drought and recovery. *J. Climate,* **21,** 3797–3814, doi:10.1175/2008JCLI2055.1.

Held, I. M., and M. J. Suarez, 1994: A proposal for the intercomparison of the dynamical cores of atmospheric general circulation models. *Bull. Amer. Meteor. Soc.,* **75,** 1825–1830, doi:10.1175/1520-0477(1994)075<1825:APFTIO>2.0.CO;2.

Horel, J. D., and J. M. Wallace, 1981: Planetary-scale atmospheric phenomena associated with the Southern Oscillation. *Mon. Wea. Rev.,* **109,** 813–829, doi:10.1175/1520-0493(1981)109<0813:PSAPAW>2.0.CO;2.

Ju, J., and J. Slingo, 1995: The Asian summer monsoon and ENSO. *Quart. J. Roy. Meteor. Soc.,* **121,** 1133–1168, doi:10.1002/qj.49712152509.

Kalnay, E., and Coauthors, 1996: The NCEP/NCAR 40-Year Reanalysis Project. *Bull. Amer. Meteor. Soc.,* **77,** 437–470, doi:10.1175/1520-0477(1996)077<0437:TNYRP>2.0.CO;2.

Kang, I.-S., E. K. Jin, and K.-H. An, 2006: Secular increase of seasonal predictability for the 20th century. *Geophys. Res. Lett.,* **33,** L02703, doi:10.1029/2005GL024499.

——, J. Kug, M.-J. Lim, and D.-H. Choi, 2011: Impact of transient eddies on extratropical seasonal-mean predictability in DEMETER models. *Climate Dyn.,* **37,** 509–519, doi:10.1007/s00382-010-0873-4.

——, H.-H. No, and F. Kucharski, 2014: ENSO amplitude modulation associated with the mean SST changes in the tropical central Pacific induced by Atlantic multidecadal oscillation. *J. Climate,* **27,** 7911–7920, doi:10.1175/JCLI-D-14-00018.1.

Keenlyside, N. S., H. Ding, and M. Latif, 2013: Potential of equatorial Atlantic variability to enhance El Niño prediction. *Geophys. Res. Lett.,* **40,** 2278–2283, doi:10.1002/grl.50362.

Kinter, J. L., K. Miyakoda, and S. Yang, 2002: Recent change in the connection from the Asian monsoon to ENSO. *J. Climate,* **15,** 1203–1215, doi:10.1175/1520-0442(2002)015<1203:RCITCF>2.0.CO;2.

Krishna Kumar, K., B. Rajagopalan, and M. A. Cane, 1999: On the weakening of relationship between the Indian monsoon and ENSO. *Science,* **284,** 2156–2159, doi:10.1126/science.284.5423.2156.

Krishnamurthy, V., and B. N. Goswami, 2000: Indian monsoon–ENSO relationship on interdecadal timescale. *J. Climate,* **13,** 579–595, doi:10.1175/1520-0442(2000)013<0579:IMEROI>2.0.CO;2.

Kucharski, F., F. Molteni, and A. Bracco, 2006: Decadal interactions between the western tropical Pacific and the North Atlantic Oscillation. *Climate Dyn.,* **26,** 79–91, doi:10.1007/s00382-005-0085-5.

——, A. Bracco, J. H. Yoo, and F. Molteni, 2007: Low-frequency variability of the Indian monsoon–ENSO relationship and the tropical Atlantic: The ''weakening'' of the 1980s and 1990s. *J. Climate,* **20,** 4255–4266, doi:10.1175/JCLI4254.1.

——, F. Molteni, M. P. King, R. Farneti, I.-S. Kang, and L. Feudale, 2013a: On the need of intermediate complexity general circulation models: A ''SPEEDY'' example. *Bull. Amer. Meteor. Soc.,* **94,** 25–30, doi:10.1175/BAMS-D-11-00238.1.

——, N. Zeng, and E. Kalnay, 2013b: A further assessment of vegetation feedback on decadal Sahel rainfall variability. *Climate Dyn.,* **40,** 1453–1466, doi:10.1007/s00382-012-1397-x.

Kumar, P., K. Rupa Kumar, M. Rajeevan, and A. K. Sahai, 2007: On the recent strengthening of the relationship between ENSO and northeast monsoon rainfall over South Asia. *Climate Dyn.,* **28,** 649–660, doi:10.1007/s00382-006-0210-0.

López-Parages, J., and B. Rodríguez-Fonseca, 2012: Multidecadal modulation of El Niño influence on the Euro-Mediterranean

rainfall. *Geophys. Res. Lett.,* **39,** L02704, doi:10.1029/2011GL050049.

——, and Coauthors, 2013: Nonstationary interannual teleconnections modulated by multidecadal variability. *Fis. Tierra,* **25,** 11–39, doi:10.5209/rev_FITE.2013.v25.43433.

Losada, T., B. Rodríguez-Fonseca, I. Polo, S. Janicot, S. Gervois, F. Chauvin, and P. Ruti, 2010: Tropical response to the Atlantic equatorial mode: AGCM multimodel approach. *Climate Dyn.,* **35,** 45–52, doi:10.1007/s00382-009-0624-6.

——, ——, E. Mohino, J. Bader, S. Janicot, and C. R. Mechoso, 2012: Tropical SST and Sahel rainfall: A non-stationary relationship. *Geophys. Res. Lett.,* **39,** L12705, doi:10.1029/2012GL052423.

Martín-Rey, M., B. Rodríguez-Fonseca, I. Polo, and F. Kucharski, 2014: On the Atlantic–Pacific Niños connection: A multidecadal modulated mode. *Climate Dyn.,* **43,** 3163–3178, doi:10.1007/s00382-014-2305-3.

Mohino, E., S. Janicot, and J. Bader, 2011: Sahel rainfall and decadal to multi-decadal sea surface temperature variability. *Climate Dyn.,* **37,** 419–440, doi:10.1007/s00382-010-0867-2.

Molteni, F., 2003: Atmospheric simulations using a GCM with simplified physical parameterizations. I: Model climatology and variability in multi-decadal experiments. *Climate Dyn.,* **20,** 175–191, doi:10.1007/s00382-002-0268-2.

Palmer, T. N., and Coauthors, 2004: Development of a European multimodel ensemble system for seasonal-to-interannual prediction (DEMETER). *Bull. Amer. Meteor. Soc.,* **85,** 853–872, doi:10.1175/BAMS-85-6-853.

Rasmusson, E. M., and T. H. Carpenter, 1983: The relationship between the eastern Pacific sea surface temperature and rainfall over India and Sri Lanka. *Mon. Wea. Rev.,* **111,** 517–528, doi:10.1175/1520-0493(1983)111<0517:TRBEEP>2.0.CO;2.

Rodríguez-Fonseca, B., I. Polo, J. García-Serrano, T. Losada, E. Mohino, C. R. Mechoso, and F. Kucharski, 2009: Are Atlantic Niños enhancing Pacific ENSO events in recent decades? *Geophys. Res. Lett.,* **36,** L20705, doi:10.1029/2009GL040048.

Rowell, D. P., C. K. Folland, K. Maskell, and M. N. Ward, 1995: Variability of summer rainfall over tropical North Africa (1906–92): Observations and modelling. *Quart. J. Roy. Meteor. Soc.,* **121,** 669–704, doi:10.1002/qj.49712152311.

Schneider, U., A. Becker, P. Finger, A. Meyer-Christoffer, M. Ziese, and B. Rudolf, 2014: GPCC's new land surface precipitation climatology based on quality-controlled in situ data and its role in quantifying the global water cycle. *Theor. Appl. Climatol.,* **115,** 15–40, doi:10.1007/s00704-013-0860-x.

Smith, T. M., and R. W. Reynolds, 2003: Extended reconstruction of global sea surface temperature based on COADS data (1854–1997). *J. Climate,* **16,** 1495–1510, doi:10.1175/1520-0442-16.10.1495.

——, ——, T. C. Peterson, and J. Lawrimore, 2008: Improvements to NOAA's historical merged land–ocean surface temperature analysis (1880–2006). *J. Climate,* **21,** 2283–2296, doi:10.1175/2007JCLI2100.1.

Timmermann, A., and Coauthors, 2007: The influence of a weakening of the Atlantic meridional overturning circulation on ENSO. *J. Climate,* **20,** 4899–4919, doi:10.1175/JCLI4283.1.

Torrence, C., and P. J. Webster, 1999: Interdecadal changes in the ENSO–monsoon system. *J. Climate,* **12,** 2679–2690, doi:10.1175/1520-0442(1999)012<2679:ICITEM>2.0.CO;2.

Turner, A. G., P. M. Inness, and J. M. Slingo, 2007: The effect of doubled CO_2 and model basic state biases on the monsoon–ENSO system. I: Mean response and interannual variability. *Quart. J. Roy. Meteor. Soc.,* **133,** 1143–1157, doi:10.1002/qj.82.

Wallace, J. M., and D. S. Gutzler, 1981: Teleconnections in the geopotential height field during the Northern Hemisphere winter. *Mon. Wea. Rev.,* **109,** 784–812, doi:10.1175/1520-0493(1981)109<0784:TITGHF>2.0.CO;2.

Wang, B., I.-S. Kang, and J. Y. Lee, 2004: Ensemble simulations of Asian–Australian monsoon variability by 11 AGCMs. *J. Climate,* **17,** 803–818, doi:10.1175/1520-0442(2004)017<0803:ESOAMV>2.0.CO;2.

——, and Coauthors, 2009: Advance and prospectus of seasonal prediction: Assessment of the APCC/CliPAS 14-model ensemble retrospective seasonal prediction (1980–2004). *Climate Dyn.,* **33,** 93–117, doi:10.1007/s00382-008-0460-0.

Webster, P. J., and S. Yang, 1992: Monsoon and ENSO: Selectively interactive systems. *Quart. J. Roy. Meteor. Soc.,* **118,** 877–926, doi:10.1002/qj.49711850705.

——, A. M. Moore, J. P. Loschnigg, and R. R. Leben, 1999: Coupled ocean–atmosphere dynamics in the Indian Ocean during 1997–98. *Nature,* **401,** 356–360, doi:10.1038/43848.

Yadav, R. K., K. Rupa Kumar, and M. Rajeevan, 2009: Increasing influence of ENSO and decreasing influence of AO/NAO in the recent decades over northwest India winter precipitation. *J. Geophys. Res.,* **114,** D12112, doi:10.1029/2008JD011318.

——, J. H. Yoo, F. Kucharski, and M. A. Abid, 2010: Why is ENSO influencing northwest India winter precipitation in recent decades? *J. Climate,* **23,** 1979–1993, doi:10.1175/2009JCLI3202.1.

Zeng, N., and J. Yoon, 2009: Expansion of the world's deserts due to vegetation-albedo feedback under global warming. *Geophys. Res. Lett.,* **36,** L17401, doi:10.1029/2009GL039699.